

**On the predominant mechanisms active during the high
power diode laser modification of the wettability
characteristics of an $\text{SiO}_2/\text{Al}_2\text{O}_3$ -based ceramic material**

J. Lawrence

Manufacturing Engineering Division, School of Mechanical & Production Engineering, Nanyang
Technological University (NTU), Nanyang Avenue, Singapore 639798.

Correspondence

Dr. Jonathan Lawrence,
Manufacturing Engineering Division,
School of Mechanical & Production Engineering,
Nanyang Technological University (NTU),
Nanyang Avenue,
Singapore 639798.

Tel : (65) 6790 5542

Fax : (65) 6791 1859

e-mail: mjlawrence@ntu.edu.sg

Abstract

The mechanisms responsible for modifications to the wettability characteristics of a $\text{SiO}_2/\text{Al}_2\text{O}_3$ -based ceramic material in terms of a test liquid set comprising of human blood, human blood plasma, glycerol and 4-octanol after high power diode laser (HPDL) treatment have been elucidated. Changes in the contact angle, θ , and hence the wettability characteristics of the $\text{SiO}_2/\text{Al}_2\text{O}_3$ -based ceramic were attributed primarily to: modifications to the surface roughness of the ceramic resulting from HPDL interaction which accordingly effected reductions in θ , the increase in the surface O_2 content of the ceramic after HPDL treatment; since an increase in surface O_2 content intrinsically brings about a decrease in θ , and vice versa and the increase in the polar component of the surface energy, γ_{sv}^p due to the HPDL induced surface melting and resolidification which consequently created a partially vitrified microstructure that was seen to augment the wetting action. However, the degree of influence exerted by each mechanism was found to differ markedly. Isolation of each of these mechanisms permitted the magnitude of their influence to be qualitatively determined. Surface energy, by way of microstructural changes, was found to be by far the most predominant element governing the wetting characteristics of the $\text{SiO}_2/\text{Al}_2\text{O}_3$ -based ceramic. To a much lesser extent, surface O_2 content, by way of process gas, was also seen to influence to a changes in the wettability characteristics of the $\text{SiO}_2/\text{Al}_2\text{O}_3$ -based ceramic, whilst surface roughness was found to play a minor role in inducing changes in the wettability characteristics.

Keywords: high power diode laser (HPDL); vitrification; melting; wettability; surface energy

1. Introduction

The interfacial phenomena of wetting is often the predominant factor governing whether or not a coating will adhere and bond to a substrate. Although the literature abounds with studies to investigate the phenomena, most are primarily concerned with the wettability of zirconia and other oxide ceramics on metals (Chidambaram *et al.* 1992; Li 1992; Li 1995; Nikopoulos & Sotiropoulou 1987; Ueki *et al.* 1986), as well as the adhesion of silicone sealants to aluminium (Gutowski *et al.* 1992) and the coating of aluminium alloys with ceramic materials (Zhou & DeHosson 1993; Zhou & DeHosson 1994). The interfacial mechanisms investigated have focused mainly on the thermodynamic criterion (Chidambaram *et al.* 1992; Li 1995; Nikopoulos & Sotiropoulou 1987), the electronic theory (Li 1992) and the occurrence of oxidation (Ueki *et al.* 1986; Li 1993).

There is a growing amount of published work that testifies to the potential of lasers for altering the surface properties of materials in order to improve their wettability characteristics. The well documented fact that generated oxide layers often promote metal/oxide wetting has been reported by Zhou & DeHosson (1993; 1994) as a result of work on the laser coating of aluminium alloys with ceramic material. Bahnert and Bahnert *et al.* (1993; 1993), have observed and comprehensively detailed the changes in technical properties of various textile fibres, including adhesion and wetting properties, with a view to developing an alternative to the conventional methods of chemical agents addition or wet-chemical pre-processing. In recent years the excimer laser has been employed to precisely control and later the surface characteristics of a number of polymer materials. Much research has been carried out to study the effects of excimer laser radiation on the wettability characteristics of polyethylene terephthalate (PET) in both film (Heitz *et al.* 1994), fibre (Watanabe *et al.* 1993) and sheet (Andrew *et al.* 1983) form, as well as polyparaphenylene terephthalamide (PPTA) (Watanabe *et al.* 1994). Laurens *et al.* (1998; 2000) concluded that a more polar surface resulted from the excimer laser treatment of polyether-etherketon (PEEK). Comprehensive and detailed investigations by Song & Netravali (1998; 1998¹; 1999) into the effects of excimer laser radiation on the interfacial characteristics of UHSPE fibres and epoxy resin revealed a considerable increase in the interfacial shear strength resulted after laser treatment. Furthermore, Heitz *et al.* (1994), Henari & Blau (1995) and Olfert *et al.* (1996) have found that excimer laser treatment of metals results in improved coating adhesion.

But, the reasons for the changes in the wetting characteristics with regard to changes in the material's surface topography, surface composition and surface energy have not been reported on in great deal in any of the previous studies. However, Lawrence and Li have amply demonstrated the practicability of employing different types of lasers to effect changes in the wettability characteristics of ceramics (1998; 1999; 1999¹) metals (1999²; 2000) and polymers (2001) for improved adhesion and bonding, as well as comprehensively examining the changes in the wettability characteristics of the materials in terms of surface topography, surface composition and surface energy. This paper aims not only to describe a technique whereby a high power diode laser (HPDL) beam was used to alter the wettability characteristics of an SiO₂/Al₂O₃-based ceramic material, but to elucidate and give a greater understanding of the basic process phenomena and the numerous factors involved. In particular, knowledge of the predominant influential mechanisms, namely topography, microstructure and surface chemistry, and the individual effects thereof on the HPDL modified wettability characteristics of metals is established. This work describes the employment of a number of techniques to isolate these elements, thereby allowing their singular effect on changes to the wettability characteristics of the SiO₂/Al₂O₃-based ceramic treated with the HPDL to be ascertained.

2. Theoretical background

2.1. Contact angle and wettability

When a drop of liquid is placed on a solid surface it may remain as a spherical drop, or spread to cover (wet) the solid surface (Fowkes 1964). The angle with which the liquid subtends the solid is known as the contact angle. In practice, for wetting to occur the contact angle is less than 90°. If the contact angle is greater than 90° then the liquid does not wet the solid and no adhesion occurs (Fowkes 1964). When a drop of liquid is brought into contact with a flat solid surface, the final shape taken by the drop, and thus whether it will wet the surface or not, depends upon the relative magnitudes of the molecular forces that exist within the liquid (cohesive) and between the liquid and the solid (adhesive) (Fowkes 1964). The index of this effect is the contact angle θ , which the liquid subtends with the solid. θ is related to the solid and liquid surface energies, γ_{sv} and γ_{lv} , and the solid-liquid interfacial energy γ_{sl} , through the principle of virtual work expressed by the rearranged Young's equation:

$$\cos \theta = \frac{\gamma_{sv} - \gamma_{sl}}{\gamma_{lv}} \quad (1)$$

Clearly, to achieve wetting γ_{sv} should be large, while γ_{sl} and γ_{lv} should be small. Hence liquids of a lower surface tension will always spread over a solid surface of higher surface tension in order to reduce the total free-energy of the system (Zisman 1964). This is on account of the fact that the molecular adhesion between solid and liquid is greater than the cohesion between the molecules of the liquid (Fowkes 1964).

The adhesion energy of a liquid to a solid surface (the work of adhesion) W_{ad} , is given by the Young-Dupre equation:

$$W_{ad} = \gamma_{lv}(1 + \cos \theta) \quad (2)$$

2.2. Surface energy and the polar/dispersive characteristics

The intermolecular attraction which is responsible for surface energy, γ , results from a variety of intermolecular forces whose contribution to the total surface energy is additive (Fowkes 1964). The majority of these forces are functions of the particular chemical nature of a certain material, and as such the total surface energy comprises of γ^p (polar or non-dispersive interaction) and γ^d (dispersive component; since van der Waals forces are present in all systems regardless of their chemical nature). Therefore, the surface energy of any system can be described by (Fowkes 1964)

$$\gamma = \gamma^d + \gamma^p \quad (3)$$

Similarly, W_{ad} can be expressed as the sum of the different intermolecular forces that act at the interface (Fowkes 1964):

$$W_{ad} = W_{ad}^d + W_{ad}^p = 2(\gamma_{sv}^d \gamma_{lv}^d)^{1/2} + 2(\gamma_{sv}^p \gamma_{lv}^p)^{1/2} \quad (4)$$

By equating Equation (4) with Equation (2), the contact angle for solid-liquid systems can be related to the surface energies of the respective liquid and solid by

$$\cos \theta = \frac{2(\gamma_{sv}^d \gamma_{lv}^d)^{1/2} + 2(\gamma_{sv}^p \gamma_{lv}^p)^{1/2}}{\gamma_{lv}} - 1 \quad (5)$$

3. Experimental procedures

3.1 Materials

The SiO₂/Al₂O₃-based ceramic material investigated in this work is a novel composition that is used in a HPDL-based two stage ceramic tile grout sealing process (Lawrence *et al.* 1998; ¹1998). The ceramic consisted of mixed vitrifiable oxide powders: SiO₂ (53wt%); Al₂O₃ (42wt%); Fe₂O₃ (2wt%); MgO (1.5wt%); ZrO₂ (1wt%) and ZnO (0.5wt%). The oxide powders were sieved to ensure a particle size of less than 75 µm, then thoroughly mixed together to ensure homogeneity, along with approximately 50wt.% diluted sodium silicate solution so as to form a manageable paste. The compound mixture was then pasted on to an ordinary Portland cement (OPC) substrate to a thickness of 2 mm and allowed to cure at room temperature for 12 h whereupon it was irradiated with the HPDL beam. In order to carry out analytical analyses of the untreated and HPDL treated specimens, they were sectioned with a cutting machine (Struers, Ltd.) using a diamond rimmed cutting blade, and then polished using cloths and diamond suspension pastes down to 1 µm. The sectioned samples were then examined using optical microscopy, scanning electron microscopy (SEM), energy disperse X-ray analysis (EDX) and X-ray diffraction (XRD) techniques.

3.2 Laser processing procedure

A HPDL (Diomed Ltd.) emitting at 810 ±20 nm and operating in the CW mode with rated optical powers ranging from 0-60 W was used in this study. The HPDL beam was delivered to the work area by means of an optical fibre 4 m long, and of 600 µm core diameter, the end of which was connected to a 2:1 focusing lens assembly mounted on the z-axis of a 3-axis CNC gantry table. The SiO₂/Al₂O₃-based ceramic was irradiated using the defocused high order mode HPDL beam with a beam spot diameter of 1.75 mm and laser powers (measured at the workpiece using a Power Wizard power meter) of 20-55 W. A schematic illustration of the laser processing experimental arrangement is given in Figure 1. Here it can be seen that the defocused HPDL beam was fired across the surface of the SiO₂/Al₂O₃-based ceramic by traversing the samples beneath the laser beam using the x- and y-axis of the CNC gantry table at speeds ranging from 300 to 480 mm min⁻¹. So as to investigate the effects of process gas type, 3 l min⁻¹ of coaxially blown Ar, N₂ and O₂ process gas were employed.

3.3 Wetting and surface energy characterisation procedure

To examine the wetting and surface energy characteristics of the SiO₂/Al₂O₃-based ceramic and hence quantify any surface energy changes in the SiO₂/Al₂O₃-based resulting from HPDL interaction, a series of control experiments were carried out using the sessile drop technique with a variety of liquids with known surface energy properties. The control test liquids were: human blood; human blood plasma; glycerol and 4-octanol. The test liquids, along with their total surface energy (γ_2) as well as the dispersive (γ_{lv}^d) and polar (γ_{lv}^p) components, are detailed in Table 1. This particular test liquid series was selected because it has been shown in previous studies (Agathopoulos & Nikopoulos 1995; Lawrence & Li 1998; 1999; 1999¹) to be most suitable for ceramic materials such as the SiO₂/Al₂O₃-based ceramic studied in this work. The experiments were conducted in normal atmospheric conditions at a temperature of 20°C ± 2°C with the temperature of the liquids themselves throughout the experiments also being maintained at around 20°C. The droplets were released onto the surface of the test SiO₂/Al₂O₃-based ceramic substrate (treated and untreated) from the tip of a micropipette, with the resultant volume of the drops being approximately 6 x 10⁻³ cm³. Each experiment lasted for three minutes with profile photographs of the sessile drops being obtained every minute and the contact angle subsequently being measured. The standard deviation due to experimental error was calculated as being ±0.2°.

4. The general effects of high power diode laser radiation on the wettability characteristics of the SiO₂/Al₂O₃-based ceramic material

The oxide compounds of the SiO₂/Al₂O₃-based ceramic were bound together through mixing with 50wt% diluted sodium silicate solution. Sodium silicate solution (waterglass) is a viscous colourless solution of colloidal sodium silicate that, when combined with other solutions such as the SiO₂/Al₂O₃-based ceramic, forms a gel-like mass of silicate hydrate. Such a mass remains soft and malleable until it is exposed to CO₂ gas, either by means of a gas jet or through contact with the atmosphere (DeGarmo *et al.* 1997). Exposure of the hardened mass, however, to water results in a reversing of the process and the mass returns to a gel-like state. Heating of the hardened SiO₂/Al₂O₃-based ceramic mass fires the waterglass (similar to that of a ceramic material) (DeGarmo *et al.* 1997), increasing its strength and enabling it to withstand water exposure. So, exposure of the SiO₂/Al₂O₃-based ceramic to HPDL radiation results in rapid heating of the surface, for most materials typically

10^3 to 10^5 K s^{-1} (Steen 1991). This will lead to the sintering of the $\text{SiO}_2/\text{Al}_2\text{O}_3$ -based ceramic surface with the removal of the pores between the starting particles of the compound, combined with growth together and strong bonding between adjacent particles (Richerson 1992), thus a much more consolidated surface is created.

An optical micrograph of a sessile drop of a solidified vitreous enamel (20°C) placed on the surface of the $\text{SiO}_2/\text{Al}_2\text{O}_3$ -based ceramic before (a) and after (b) HPDL irradiation with θ superimposed is shown in Figure 2. The experimental results showed that throughout the period of cooling of the enamel, from the molten state at 600°C to the solid state at room temperature, no discernible change in the magnitude of the θ took place during the time of the experiments. This observation indicates that thermodynamic equilibrium was established at the solid-liquid interface at the outset of the experiment (Agathopoulos & Nikopoulos 1995). Figure 2 shows clearly that prior to HPDL interaction, it was not possible to fire the enamel onto the surface of the $\text{SiO}_2/\text{Al}_2\text{O}_3$ -based ceramic since θ was measured as 118° , and as such would prevent the enamel from wetting the $\text{SiO}_2/\text{Al}_2\text{O}_3$ -based ceramic surface. Indeed, HPDL interaction with the enamel when placed on the untreated $\text{SiO}_2/\text{Al}_2\text{O}_3$ -based ceramic surface simply resulted in the ‘balling’ of the enamel, that is the formation of small spheres approximately the diameter of the laser beam itself (Bourell *et al.* 1992; Agarwala *et al.* 1995). Furthermore, as is evident from Table 2, under the experimental laser parameters employed and processing in an O_2 atmosphere, HPDL irradiation of the surface of the $\text{SiO}_2/\text{Al}_2\text{O}_3$ -based ceramic samples resulted in changes in θ . It can be seen that in general, interaction of the $\text{SiO}_2/\text{Al}_2\text{O}_3$ -based ceramic with the HPDL beam resulted in the θ between the $\text{SiO}_2/\text{Al}_2\text{O}_3$ -based ceramic and the control liquids reducing.

4.1. The effects of surface topography

The role that surface topography plays in influencing wetting characteristics is of some importance. More specifically, the aspect of surface topography that is of particular importance is substrate surface roughness, for it is this that can contribute to effect changes in θ . Rough grooves on a surface can be categorised as either radial or circular grooves. In practical terms, any rough surface can be represented by a combination of these two cases (Zhou & DeHosson 1995), with two roughness parameters being defined as the Wenzel type, D_R (Wenzel 1936) and the Cassie/Baxter type, F_R (Cassie & Baxter 1944). In the case that wetting spreads radially, as is the likely case with the

SiO₂/Al₂O₃-based ceramic, then the resulting radial contact angle, θ_{rad} , is related to the theoretical contact angle, θ_{th} , by

$$\cos \theta_{rad} = D_R (1 - F_R) \cos \theta_{th} - F_R \quad (6)$$

According to Neumann (1974), only if F_R is equal to zero, then a model similar to that for heterogeneous solid surfaces can be developed in order to account for surface irregularities, being given by a rearrangement of Wenzel's equation:

$$\gamma_{sl} = \gamma_{sv} - \left(\frac{\gamma_{lv} \cos \theta_w}{r} \right) \quad (7)$$

where, r is the roughness factor defined as the ratio of the real and apparent surface areas and θ_w is the contact angle for the wetting of a rough surface. It is important to note that Wenzel's treatment is only effective at the position of wetting triple line (Wenzel 1936). Nonetheless, it is evident from Equation (7) that if the roughness factor, r , is large, that is the solid surface is smooth, then γ_{sl} will become small, thus, a reduction in the contact angle will be inherently realised by the liquid if $\theta_w < 90^\circ$. Conversely, if $\theta_w > 90^\circ$ then the opposite will be observed. At this point it is worth remarking that other more sophisticated approaches may be taken to examine the effects of surface roughness on wetting (Palasantzas & De Hosson 2001). For this present study, however, the use of Equation (7) is quite sufficient.

Reductions in the surface roughness of the SiO₂/Al₂O₃-based ceramic were observed (using a Taylor-Hobson Surtronic 3+ profileometer) after interaction with the HPDL beam when using any of the selected process gasses. As one can see from Table 3, the reductions occasioned in surface roughness are relatively similar in value. Similar results were obtained by Nicolas *et al.* (1997), who observed that excimer laser treatment of a ZrO₂ ceramic resulted in a smoother surface. Therefore, according to Equation (3), a reduction in θ will be inherently effected. Indeed, Figure 3 shows clearly the effect of the HPDL treated SiO₂/Al₂O₃-based ceramic surface roughness on θ . For experimental purposes the liquid, selected arbitrarily was glycerol. Such results are in accord with those obtained by Feng *et al.* (1998), who noted that θ was inversely proportional to surface roughness.

4.2. The effects of process gas type

Process gas type will be significant in determining θ , since the O_2 content of a material's surface is an influential factor governing the wetting performance of the material (Ueki 1986; Li 1993). Experiments were therefore conducted to investigate the effects of using Ar, N_2 and O_2 process gasses on θ . In order to study exclusively the effects of process gas on the wettability characteristics of the SiO_2/Al_2O_3 -based ceramic, the remaining HPDL operating parameters were set such that a similar degree of melting and solidification occurred and a similar surface roughness was achieved. Wetting is governed by the first atomic layers of the surface of a material, so to determine the element content of O_2 at the surface of the SiO_2/Al_2O_3 -based ceramic, it was necessary to examine the surface using X-ray photoemission spectroscopy (XPS).

The results of the XPS analysis of the SiO_2/Al_2O_3 -based ceramic in terms of the surface O_2 content when processed with selected gasses is shown in Figure 4. As is evident from Figure 4, increases in the surface O_2 content of the SiO_2/Al_2O_3 -based ceramic after HPDL interaction were observed only when processing was carried with an O_2 processing gas. In all other instances the surface O_2 content of both materials was seen to decrease markedly. More significantly, the assertion that surface O_2 content is an important factor in determining θ is confirmed somewhat by Figure 5, in which the effects of the differences in surface O_2 content appear to have a noticeable influence on θ . It is apparent, however, from Figure 5 that the reductions in θ bear no direct relationship with the surface O_2 content results given in Figure 4. Indeed, Figure 5 shows that reductions in θ were brought about after HPDL treatment regardless of the process gas employed, with the reductions being similar in value. Nevertheless, Figure 5 shows quite clearly that the largest reduction in θ occurred when O_2 was used as the process gas and the surface O_2 content was subsequently the highest.

4.3. The effects of surface energy and its dispersive/polar attributes

According to Fowkes (1964), the dispersive component of the surface energy of the SiO_2/Al_2O_3 -based ceramic can be estimated by using Equation (5) and plotting the graph of $\cos \theta$ against $(\gamma_{lv}^d)^{1/2}/\gamma_{lv}$. Hence the value of γ_{sv}^d is estimated by the gradient $(=2(\gamma_{sv}^d)^{1/2})$ of the line which connects the origin ($\cos \theta = -1$) with the intercept point of the straight line ($\cos \theta$ against $(\gamma_{lv}^d)^{1/2}/\gamma_{lv}$) correlating the data point with the abscissa at $\cos \theta = 1$. Figure 6 shows the best-fit plot of $\cos \theta$ against $(\gamma_{lv}^d)^{1/2}/\gamma_{lv}$ according to Equation (7) for the untreated and HPDL treated SiO_2/Al_2O_3 -based ceramic (O_2 process

gas) - experimental control liquids system. Comparing the ordinate intercept points of the untreated and HPDL treated SiO₂/Al₂O₃-based ceramic(O₂ process gas) - liquid systems, it can be seen clearly from Figure 6 that for the untreated SiO₂/Al₂O₃-based ceramic (O₂ process gas) - liquid systems the best-fit straight line intercepts the ordinate closer to the origin. This observation indicates that, in principle, dispersion forces act mainly at the SiO₂/Al₂O₃-based ceramic (O₂ process gas) - liquid interfaces resulting in poor adhesion (Fowkes 1964; Chattoraj & Birdi 1984). Conversely, Figure 6 shows that the best-fit straight line for the HPDL treated SiO₂/Al₂O₃-based ceramic (O₂ process gas) - liquid systems intercepts the ordinate considerably higher above the origin. Such a finding implies the action of polar forces across the interface, in addition to dispersion forces, therefore improved wettability and adhesion is promoted (Fowkes 1964; Chattoraj & Birdi 1984).

It is not possible to determine the value of the polar component of the SiO₂/Al₂O₃-based ceramic (O₂ process gas) surface energy directly from Figure 6 on account of the intercept of the straight line ($\cos \theta$ against $(\gamma_{lv}^d)^{1/2}/\gamma_{lv}$) being at $2(\gamma_{sv}^p \gamma_{lv}^p)^{1/2}/\gamma_{lv}$ and as such, only referring to individual control liquids and not the control liquid system as a whole. All the same, it has been established that the entire amount of the surface energies owing to dispersion forces of either the solids or the liquids are active in the wettability performance (Fowkes 1964; Good & Girifalco 1960). Thus it is possible to calculate the dispersive component of the work of adhesion from Equation (4). The results reveal that for each particular control liquid in contact with both the untreated and HPDL treated SiO₂/Al₂O₃-based ceramic (O₂ process gas) surfaces, W_{ad} can be correlated with W_{ad}^d by the relationship

$$W_{ad} = aW_{ad}^d + b \quad (8)$$

Also, for the control test liquids used, a linear relationship between the dispersive and polar components of the control test liquids surface energies has been deduced which satisfies the equation

$$(\gamma_{lv}^p)^{1/2} = 1.3(\gamma_{lv}^d)^{1/2} + 1.15 \quad (9)$$

By introducing Equation (8) into Equation (6) and rearranging, then

$$W_{ad}^p = (a - 1)W_{ad}^d + b \quad (10)$$

or

$$\left(\gamma_{sv}^p\right)^{1/2}\left(\gamma_{lv}^p\right)^{1/2} = (a-1)\left(\gamma_{sv}^d\right)^{1/2}\left(\gamma_{lv}^d\right)^{1/2} + \frac{b}{2} \quad (11)$$

Further, by introducing Equation (9) into Equation (11) and differentiating with respect to $\left(\gamma_{lv}^d\right)^{1/2}$, considering that $\left(\gamma_{sv}^d\right)^{1/2}$ and $\left(\gamma_{sv}^p\right)^{1/2}$ are constant, then the following is valid:

$$\left(\gamma_{sv}^p\right)^{1/2} = \frac{\left(\gamma_{sv}^d\right)^{1/2}(a-1)}{0.45} \quad (12)$$

From a plot of Equation (12), a can be determined for the untreated and HPDL treated SiO₂/Al₂O₃-based ceramic (O₂ process gas) (1.2 and 1.7 respectively). Since γ_{sv}^d has already been determined for the untreated and HPDL treated SiO₂/Al₂O₃-based ceramic from Figure 6, then it is possible to calculate γ_{sv}^p for untreated and HPDL treated SiO₂/Al₂O₃-based ceramic (O₂ process gas) using Equation (12).

The values determined for γ_{sv}^d and γ_{sv}^p for both the untreated and HPDL treated SiO₂/Al₂O₃-based ceramic (O₂ process gas) are given in Table 4. Evidently the HPDL melting of the surface of the SiO₂/Al₂O₃-based ceramic (O₂ process gas) leads to a reduction in the total surface energy whilst increasing the polar component of the surface energy, thereby improving the action of wetting and adhesion. Such changes in the surface energy of the SiO₂/Al₂O₃-based ceramic (O₂ process gas) after HPDL melting are due to the fact partial vitrification of the surface is occasioned, a transition that is known to effect a reduction in γ_{sv} and an increase in γ_{sv}^p (Agathopoulos & Nikopoulos 1995). It is important to note that because of the long range ionic interactions in the SiO₂/Al₂O₃-based ceramic (O₂ process gas) and the composite nature of the interfaces between the SiO₂/Al₂O₃-based ceramic (O₂ process gas) and the liquids, it is highly likely that the thermodynamically defined total solid surface energy, as defined in Equation (2), will be higher than the sum of the γ^d and γ^p components of the surface energy. Indeed, the derivation that leads to Equation (5) can only be done under the specific assumption that the ionisation potentials are all equal and that dipole-dipole random orientation interactions dominate over dipole-induced dipole random interactions. Although the increase in (excess) surface free energy will probably be less than the increase in the total lattice energy. On the other hand an absorbed liquid layer may shield the ionic fields substantially. As such, all the data derived from Equations (4) - (5) and Equations (8) - (12) should be considered as being

semi-empirical. Notwithstanding this, as the studies by Gutowski *et al.* (1992) and Agathopoulos & Nikopoulos (1995) found, it is reasonable to conclude from the data obtained from Equations (8) - (12) that HPDL treatment of the $\text{SiO}_2/\text{Al}_2\text{O}_3$ -based ceramic surface (O_2 process gas) has caused an increase γ^p .

4.4. The effects of surface melting and microstructure

Such changes in the surface energy are, along with other things, brought about as a result of changes in the microstructure of the $\text{SiO}_2/\text{Al}_2\text{O}_3$ -based ceramic after HPDL interaction. From Figure 7(a) it can be seen clearly that before HPDL treatment the surface of the $\text{SiO}_2/\text{Al}_2\text{O}_3$ -based ceramic appears coarse, with individual crystals of the constituent components being clearly discernible. After laser treatment (Figure 7(b)) there is more surface ordering, with the surface appearing cellular-dendritic, showing that fusion of the individual particulates has occurred. Such a solidification structure is indicative of rapidly solidified microstructures (Kattamis 1981). Moreover, an XRD analysis of the $\text{SiO}_2/\text{Al}_2\text{O}_3$ -based ceramic surface before and after HPDL treatment (Figure 8) revealed that, on the whole, the phases present within the HPDL treated region were the same, but their proportions were different. In particular, after HPDL treatment it was not possible to detect any SiO_2 whilst the Al_2O_3 was depleted. Yet an EDX analysis showed that Si and Al were still present in similar proportions on the $\text{SiO}_2/\text{Al}_2\text{O}_3$ -based ceramic surface before and after HPDL treatment. This indicates that partial laser vitrification of the $\text{SiO}_2/\text{Al}_2\text{O}_3$ -based ceramic surface has occurred because these materials are glass forming elements, and as such, vitrified when irradiated. Additionally, it is important to note that the peaks in Figure 8 which are unmarked, for ease of analysis since they are not of direct interest, are likely to be mullite (121) and (220), which provides diffraction peaks in the range 35° to 40° . Further, some formation of spinel (MgAl_2O_4) would perhaps be expected, however, this was not detected.

It is important to determine the degree of HPDL treatment necessary to facilitate such microstructural changes which in turn bring about the surface energy changes. In particular, to establish what part melting of the $\text{SiO}_2/\text{Al}_2\text{O}_3$ -based ceramic surface plays in the promotion of wetting. Now, melting of the $\text{SiO}_2/\text{Al}_2\text{O}_3$ -based ceramic surface is the direct result of heat input resulting from the energy deposited on the surface by the HPDL beam, which is a function of certain laser operating parameters: beam spot size, power and traverse speed. So, in order to analyse the effect melting of the $\text{SiO}_2/\text{Al}_2\text{O}_3$ -based ceramic surface has on the wettability performance, a series of wetting experiments

using a vitreous enamel were conducted to determine θ for a range of energy densities. The experiments were carried with an O₂ process gas. The contact angle measurement procedure was as described earlier. The surface condition of the laser treated SiO₂/Al₂O₃-based ceramic was determined by means of SEM analysis. The relationship between θ and the energy density is shown in Figure 9.

As is clearly discernible from Figure 9, the surface condition of the HPDL treated SiO₂/Al₂O₃-based ceramic has a considerable effect on θ . Notably, Figure 9 indicates that the melting, and consequently the partial vitrification of the glass forming elements (SiO₂ and Al₂O₃) within the SiO₂/Al₂O₃-based ceramic, is a prerequisite for realising significant reductions in θ . As one can see, after the onset of melting at around 225 J cm⁻² θ reduces sharply from 113° to 33°, after which no further decrease (or increase) is discernible until the energy density exceeds 525 J cm⁻². After this point a small increase in θ from 33° to 39° was observed. This increase is probably because this energy density level lies outside of the optimum operating conditions and will therefore cause an increase in the surface roughness which, as was seen earlier, has a small but discernible effect on θ . Furthermore, the mere reordering of the crystals, rather than melting and re-solidification, that occurs at power densities below 225 J cm⁻² appears to have only a slight effect on θ , reducing it from 118° to 113°. Even so, such a reduction in θ reveals that HPDL interaction without the incidence of melting does slightly affect the wettability characteristics of the SiO₂/Al₂O₃-based ceramic.

5. Determination of the predominant mechanisms governing the high power diode laser effected modifications to the wettability characteristics of the SiO₂/Al₂O₃-based ceramic material

The preceding results and discussion demonstrate clearly that interaction of the HPDL beam with the SiO₂/Al₂O₃-based ceramic surface resulted in the contact angle formed between the control liquids altering to various degrees depending upon the laser processing parameters employed. Such changes in the value of θ are influenced primarily by: modifications to the surface roughness; changes in the surface O₂ content and changes to the surface energy characteristics of the SiO₂/Al₂O₃-based ceramic. Firstly, advantageous modifications to the surface roughness of the SiO₂/Al₂O₃-based ceramic were seen to take place regardless of the process gas used. This suggests that under the conditions used, HPDL treatment of the surface of the SiO₂/Al₂O₃-based ceramic generated an ideal amount of surface

melting and resolidification. This in turn resulted in reductions, to various degrees, in the surface roughness, thereby directly reducing θ . Secondly, changes in the surface O₂ content of the SiO₂/Al₂O₃-based ceramic resulting from HPDL treatment in the various process gas atmospheres is an influential factor in the promotion of the action of wetting. This is because an increase in surface O₂ content inherently effects a decrease in θ and vice versa. Lastly, an increase in the polar component, γ_{sv}^p , of the surface energy resulting from the melting and resolidification of the surface of the SiO₂/Al₂O₃-based ceramic occurred. This, event naturally created a different microstructure that quite possibly improved the action of wetting and adhesion.

This analysis, however, does not make it clear whether after HPDL surface treatment it is the surface roughness, the microstructural changes or the O₂ content alone, or a combination thereof, that are the principal mechanisms influencing the observed changes in the wettability characteristics of the SiO₂/Al₂O₃-based ceramic. But, by employing a strictly monitored multi-stage grinding procedure, it was possible to isolate the various influential factors detailed above and therefore analyse and qualitatively quantify the effect each one had on the wettability characteristics of the SiO₂/Al₂O₃-based ceramic. In the first stage, the surfaces of the untreated and HPDL treated SiO₂/Al₂O₃-based ceramic samples (treated in Ar, N₂ and O₂ atmospheres) were ground down to a surface roughness (Ra) of 3 μ m, whilst still retaining a HPDL treated surface. In this way it was possible to isolate the effects of surface roughness by rendering them non-effective, and investigate at least the effects of the microstructural changes (and hence surface energy) and possibly those of the O₂ content (and hence process gas effects). In order to evaluate the influence of surface roughness an intermediate grinding stage was incorporated in which the samples were ground down to 1 μ m whilst still retaining the HPDL induced microstructure. In the final stage the same SiO₂/Al₂O₃-based ceramic samples were ground down further (1 μ m) to remove the HPDL induced microstructures. Thus, one is effectively removing the effects of microstructural changes (surface energy) from the previous investigation, therefore allowing the O₂ content (process gas effects) to be studied.

An examination of the contact angle characteristics of the ground SiO₂/Al₂O₃-based ceramic samples using only human blood revealed that a large difference in θ between the HPDL treated and untreated samples was still present. For the HPDL treated samples, θ had increased slightly across the range of samples to around 39-40°, whereas θ for the untreated samples had reduced from 61° to 59°. From an XPS analysis of the O₂ content of the SiO₂/Al₂O₃-based ceramic samples, it was found that the O₂

content of the untreated sample remained around the original value of 28.1at%, whilst that of the HPDL treated samples was found to have reduced to a level similar to that of the untreated sample, 28.2-28.7at%. Since a considerable difference in the measured contact angles of the HPDL treated and untreated $\text{SiO}_2/\text{Al}_2\text{O}_3$ -based ceramic samples was still in evidence, despite grinding down the samples to a surface roughness of 3 μm , then it appears that surface roughness does not have as greater influence on the wetting characteristics of the $\text{SiO}_2/\text{Al}_2\text{O}_3$ -based ceramic than that of microstructure. The slight increase in θ for the HPDL treated $\text{SiO}_2/\text{Al}_2\text{O}_3$ -based ceramic samples is believed to be due to the reduction on the surface O_2 content. This is of importance, for such a supposition implies that surface O_2 content is more influential in determining the wetting characteristics of the $\text{SiO}_2/\text{Al}_2\text{O}_3$ -based ceramic than surface roughness.

This proposition was borne out somewhat when the samples were ground further. In this subsequent stage the samples were ground down to a surface roughness of 1 μm whilst still retaining the HPDL induced microstructure, thereby allowing a comparative analysis of the effects of surface O_2 content and surface roughness to be carried out. An XPS analysis of the O_2 content of the $\text{SiO}_2/\text{Al}_2\text{O}_3$ -based ceramic samples revealed that the O_2 content of the untreated and HPDL treated samples remained around the values obtained after the first grinding stage; for the untreated sample around the original value of 28.1at% and likewise for the HPDL treated samples at 28.1-28.7at%. The values of θ observed for the untreated and HPDL treated $\text{SiO}_2/\text{Al}_2\text{O}_3$ -based ceramic were again markedly different. As in the previous grinding stage, θ for the HPDL treated samples remained at 39-40°. On the other hand, θ for the untreated samples had reduced slightly to 58°. From this it possible to say that the conceivable reductions in θ due to reductions in the surface roughness are limited to a value well above that achieved after HPDL treatment. Moreover, since no reduction in θ for the HPDL treated $\text{SiO}_2/\text{Al}_2\text{O}_3$ -based ceramic samples was observed after generating a much smoother surface, then this reveals that surface O_2 content is indeed more instrumental in deciding the wetting characteristics of the $\text{SiO}_2/\text{Al}_2\text{O}_3$ -based ceramic than surface roughness.

After the same $\text{SiO}_2/\text{Al}_2\text{O}_3$ -based ceramic samples were ground down further (1 μm) to remove the HPDL induced microstructures, the XPS analysis showed that the surface O_2 content on the untreated and HPDL treated samples were practically the same at the original untreated value of 28.1-28.4at%. Similarly, an examination of the contact angles for the untreated and HPDL treated samples revealed that θ for the untreated $\text{SiO}_2/\text{Al}_2\text{O}_3$ -based ceramic sample remained at approximately the same value as in the previous grinding stage, 58°. More significantly, θ for the HPDL treated samples was also

consistently around the original untreated value of 58-61⁰. Basically the removal of the HPDL generated microstructure appears to have effected an increase in θ for the HPDL treated samples to the original levels, despite the generation of a much smoother surface (1 μm compared to 6.3 μm). Such findings reveal unequivocally that microstructure is by far the most predominant mechanism governing the wetting characteristics of the $\text{SiO}_2/\text{Al}_2\text{O}_3$ -based ceramic.

So, it is therefore reasonable to assume that surface energy differences brought about by microstructural changes have a more active part in deciding the wettability characteristics of the $\text{SiO}_2/\text{Al}_2\text{O}_3$ -based ceramic than either surface roughness or surface O_2 content. Furthermore, a contact angle increase, rather than a decrease, was realised for the HPDL treated $\text{SiO}_2/\text{Al}_2\text{O}_3$ -based ceramic samples when reductions in the surface O_2 were occasioned and smoother surfaces were generated simultaneously, then it is reasonable to assume that O_2 has more influence over the wettability characteristics of the $\text{SiO}_2/\text{Al}_2\text{O}_3$ -based ceramic than surface roughness.

6. Conclusions

Modification of the contact angle, θ , and hence the wettability characteristics of a $\text{SiO}_2/\text{Al}_2\text{O}_3$ -based ceramic material using a high power diode laser (HPDL) has been shown to be a feasible proposition. Such changes in the wettability characteristics of the $\text{SiO}_2/\text{Al}_2\text{O}_3$ -based ceramic were attributed primarily to the following factors. Firstly, modifications to the surface roughness resulting from HPDL interaction which, regardless of the process gas used, induced an ideal level of melting and resolidification. This in turn effected reductions to various degrees in the surface roughness from an Ra value before HPDL interaction of 25.9 μm to 6.3-6.6 μm after HPDL treatment, thereby directly reducing θ . Secondly, the 40at% increase in the surface O_2 content of the $\text{SiO}_2/\text{Al}_2\text{O}_3$ -based ceramic after HPDL treatment in the various process gas atmospheres; since an increase in surface O_2 content intrinsically brings about a decrease in θ , and vice versa. Finally, the semi-empirically determined increase in the polar component of the surface energy, γ_{sv}^p , of the $\text{SiO}_2/\text{Al}_2\text{O}_3$ -based ceramic (O_2 process gas) from an original value of 2.0 mJ/m^2 to 16.2 mJ/m^2 . This increase was the result of the HPDL induced surface melting and resolidification which consequently created a partially vitrified microstructure that was seen to augment the action of wetting and adhesion.

Work was conducted to isolate each of these mechanisms, thereby allowing the magnitude of their influence to be qualitatively determined. The degree of influence exerted by each factor was found to

differ considerably. From the analysis, surface energy, by way of microstructural changes, was found to be by far the most predominant mechanism governing the wetting characteristics of the $\text{SiO}_2/\text{Al}_2\text{O}_3$ -based ceramic. To a much lesser extent, surface O_2 content, by way of process gas, was also seen to influence to a changes in the wettability characteristics of the $\text{SiO}_2/\text{Al}_2\text{O}_3$ -based ceramic, whilst surface roughness was found to play a minor role in inducing changes in the wettability characteristics. Furthermore, based on the findings of this study, it is not unreasonable to assert that the results are generic and could therefore be applied to many ceramic materials of a similar nature in terms of wettability characteristics modification by means of HPDL radiation.

Acknowledgements

The author would like to express his gratitude to Prof. Lin Li of the Laser Processing Research Centre in UMIST for allowing him to use the high power diode laser. Many thanks also to the numerous members of staff at UMIST and NTU who assisted the author in the analytical analysis required for this work.

References

- Agarwala, M. Bourell, D.L. Beaman, J.J. Marcus, H.L. & Barlow, J.W. 1995 *Rapid Prototyping J.* **1**, 26-36.
- Agathopoulos, S. & Nikolopoulos, P. 1995 *J. of Biomed. Mater. Res.* **29**, 421-429.
- Andrew, J.E. Dyer, P.E. Forster, D. & Key, P.H. 1983 *Appl. Phys. Lett.* **43**, 717-718.
- Bahners, T. Kesting, W. & Schollmeyer, E. 1993 *Appl. Surf. Sci.* **69**, 12-15.
- Bahners, T. 1993 *Opt. Quan. Elec.* **27**, 1337-1348.
- Bourell, D.L. Marcus, H.L. Barlow, J.W. & Beaman, J.J. 1992 *Int. J. Powder Metall.* **28**, 369-381.
- Cassie, A.B.D. & Baxter, S. 1944 *Trans. Faraday Soc.* **40**, 546-552.
- Chattoraj, D.K. & Birdi, K.S. 1984 *Adsorption and the Gibbs surface excess*. New York: Plenum Press.
- Chidambaram, P.R. Edwards, G.R. & Olson, D.L. 1992 *Mater. Trans. B* **23**, 215-222.
- DeGarmo, E.P. Black, J.T. & Kohser, R.A. 1997 *Materials and processes in manufacturing*, Upper Saddle River: Prentice Hall.
- Feng, A. McCoy, B.J. Munir, Z.A. & Cagliostro, D. 1998 *Mat. Sci. & Eng. A* **1**, 50-56.
- Fowkes, F.M. 1964 *Ind. Eng. Chem.* **56**, 40-52.
- Good, R.J. & Girifalco, L.A. 1960 *J. Phys. Chem.* **64**, 561-565.
- Gutowski, W.W. Russell, L. & Cerra, A. 1992 Adhesion of silicone sealants to organic-coated aluminium. In *Science and technology of building seals, sealants, glazing and waterproofing* (Ed. J.M. Klosowski), pp 144-159. Philadelphia: ASTM.
- Heitz, J. Arenholz, E. Kefer, T. Bäuerle, D. Hibst, H. & Hagemeyer, A. 1992 *Appl. Phys. A* **55**, 391-392.
- Henari, F. & Blau, W. 1995 *Appl. Optics* **34**, 581-584.
- Kattamis, T.Z. 1981 *Lasers in metallurgy*. New York: AMIE.
- Laurens, P. Sadras, B. Decobert, F. Arefiknonsari, F. & Amouroux, J. 1998 *Int. J. Adhesion Adhesives* **18**, 19-27.

- Laurens, P. Ould Bouali, B. Meducin, F. & Sadras, B. 2000 *Appl. Surf. Sci.* **154/155**, 658-663.
- Lawrence, J. Li, L. & Spencer, J.T. 1998 Comparison of beam interaction characteristics of an alumina/silica-based oxide and an enamel for CO₂, Nd:YAG and high power diode lasers. In: *Proc. of ICALEO'98: Laser Materials Processing*, Vol 857B, pp. 76-85. Orlando: Laser Institute of America.
- Lawrence, J. Li, L. & Spencer, J.T. 1998 *Optics Laser Tech.* **30**, 205-214.
- ¹Lawrence, J. Li, L. & Spencer, J.T. 1998 *Optics Laser Tech.* **30**, 215-223.
- Lawrence, J. & Li, L. 1999 *J. Phys. D* **32**, 1075-1082.
- ¹Lawrence, J. & Li, L. 1999 *Appl. Surf. Sci.* **138/139**, 388-393.
- ²Lawrence, J. & Li, L. 1999 *J. Phys. D* **32**, 2311-2318.
- Lawrence, J. & Li, L. 2000 *Appl. Surf. Sci.* **154/155**, 664-669.
- Lawrence, J. & Li, L. 2001 *Mater. Sci. Eng. A.* **303**, 142-149.
- Li, J.G. 1992 *J. Mater. Sci. Lett.* **11**, 903-905.
- Li, J.G. 1993 *Rare Met.* **2**, 84-96.
- Li, J.G. 1995 *Mater. Lett.* **22**, 169-174.
- Palasantzas, G. & De Hosson, J. Th. M. 2001 *Acta Mater.* **49**, 3533-3538.
- Neumann, A., W. 1974 *Adv. Colloid Interface Sci.* **4**, 438.
- Nicolas, G. Autric, M. Marine, W. & Shafeev, G.A. 1997 *Appl. Surf. Sci.* **109/110**, 289-292.
- Nikopoulos, P. & Sotiropoulou, D. 1987 *J. Mater. Sci. Lett.* **6**, 1429-1430.
- Olfert, M. Duley, W. & North, T. 1996 Surface treatment and film deposition. In *Laser processing* (Eds. J. Mazumder, O. Conde, R. Villan and W. M. Steen), pp. 479-490. Amsterdam: Kluwer Academic Publishers.
- Richerson, D.W. 1992 *Modern ceramic engineering*, New York: Dekker.
- Song, Q. & Netravali, A.N. 1998 *J. Adhesion Sci. Tech.* **9**, 957-982.
- ¹Song, Q. & Netravali, A.N. 1998 *J. Adhesion Sci. Tech.* **9**, 983-998.
- Song, Q. & Netravali, A.N. 1999 *J. Adhesion Sci. Tech.* **13**, 501-516.
- Steen, W.M. 1991 *Laser materials processing*. London: Springer-Verlag.

- Ueki, M. Naka, M. & Okamoto, I. 1986 *J. Mater. Sci. Lett.* **5**, 1261-1262.
- Watanabe, H. Shimizu, H. & Takata, T. 1993 *Sen'-i Gakkaishi* **49**, 616-623.
- Watanabe, H. & Takata, T. 1994 *J. Adhesion Sci. Tech.* **8**, 1425-1438.
- Wenzel, R.N. 1936 *Ind. Eng. Chem.* **28**, 988- 994.
- Zhou, X.B. & DeHosson, J.T.M. 1993 *J. de Phys. IV* **3**, 1007-1011.
- Zhou, X.B. & DeHosson, J.T.M 1994 *Acta Metall. Mater.* **42**, 1155-1162.
- Zhou, X.B. & DeHosson, J.T.M 1995 *J. Mat. Research* **10**, 1984-1992.
- Zisman, W.A. 1964 Contact angle, wettability and adhesion. In: *Advances in chemistry Series 43* (Ed. R.F. Gould), pp 1-51. Washington DC: American Chemical Society.

Figure 1

Schematic diagram of the experimental set-up for the HPDL treatment of the $\text{SiO}_2/\text{Al}_2\text{O}_3$ -based ceramic.

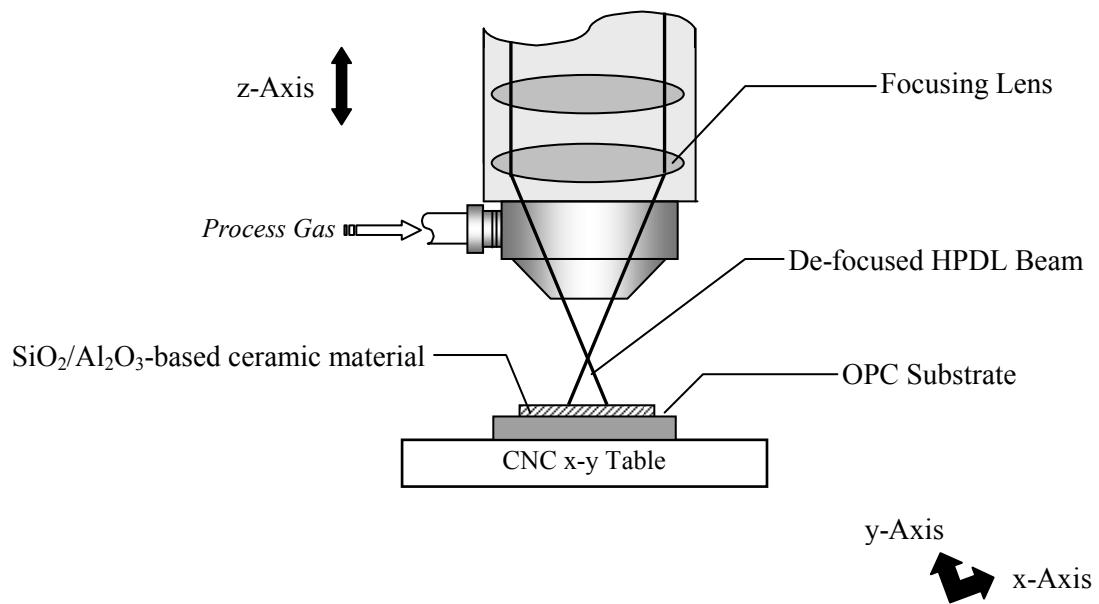
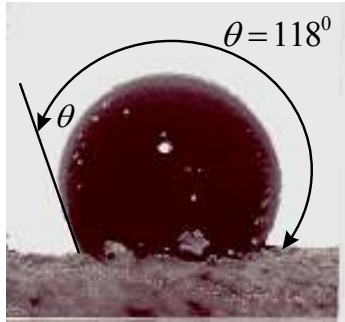
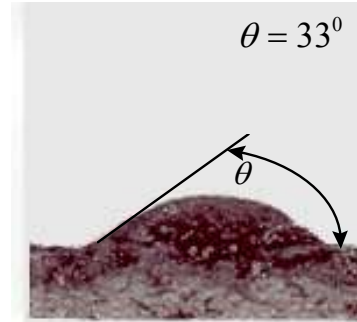


Figure 2

Contact angles (θ) for a fired vitreous enamel on (a) the untreated surface and (b) the HPDL treated surface of the $\text{SiO}_2/\text{Al}_2\text{O}_3$ -based ceramic material.



(a)



(b)

Figure 3

Relationship between the HPDL treated $\text{SiO}_2/\text{Al}_2\text{O}_3$ -based ceramic material contact angle (θ) and surface roughness (Ra).

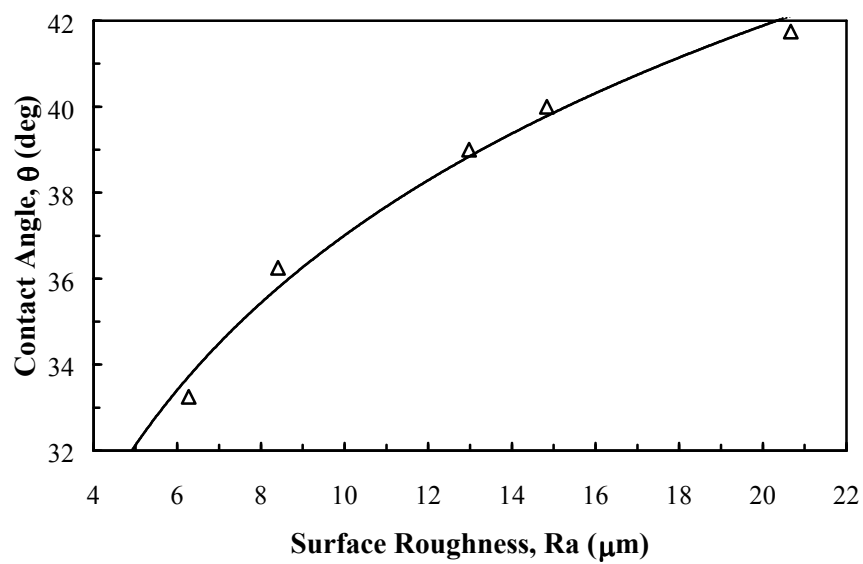


Figure 4

Surface O₂ content of the SiO₂/Al₂O₃-based ceramic material before and after HPDL surface treatment in the various process gas environments (40 W laser power and 360 mm min⁻¹ traverse speed).

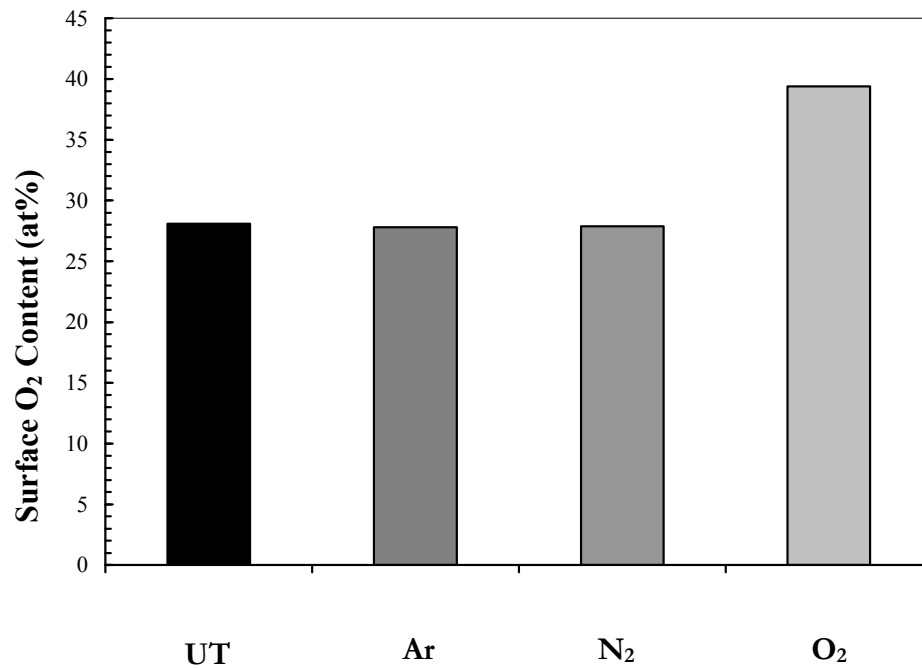


Figure 5

Mean values of contact angle (θ) formed between glycerol at 20⁰C and the SiO₂/Al₂O₃-based ceramic material before and after HPDL surface treatment in the various process gas environments (40 W laser power and 360 mm min⁻¹ traverse speed).

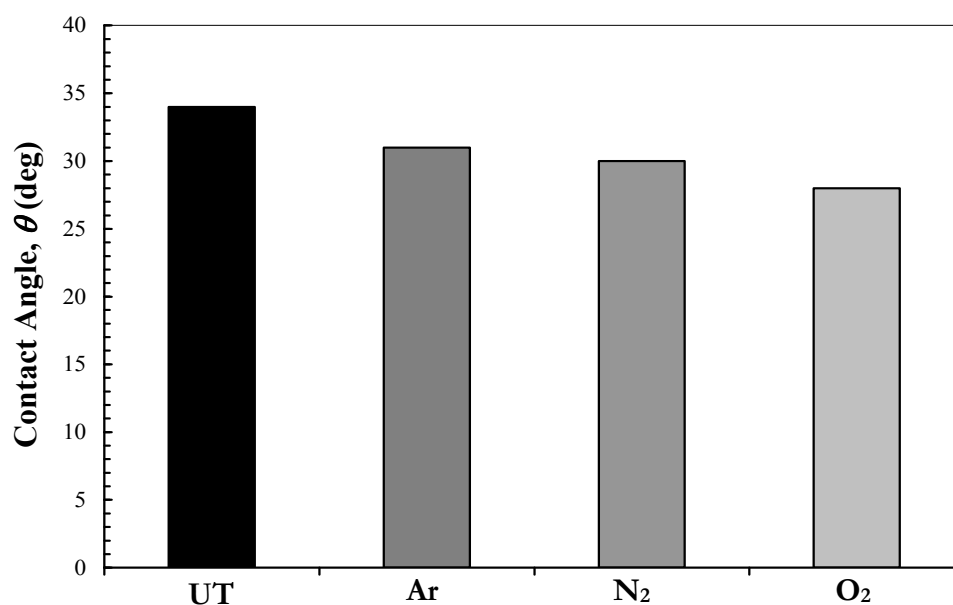


Figure 6

Plot of $\cos \theta$ against $(\gamma_{lv}^d)^{1/2} / \gamma_{lv}$ for the $\text{SiO}_2/\text{Al}_2\text{O}_3$ -based ceramic material in contact with the wetting test control liquids.

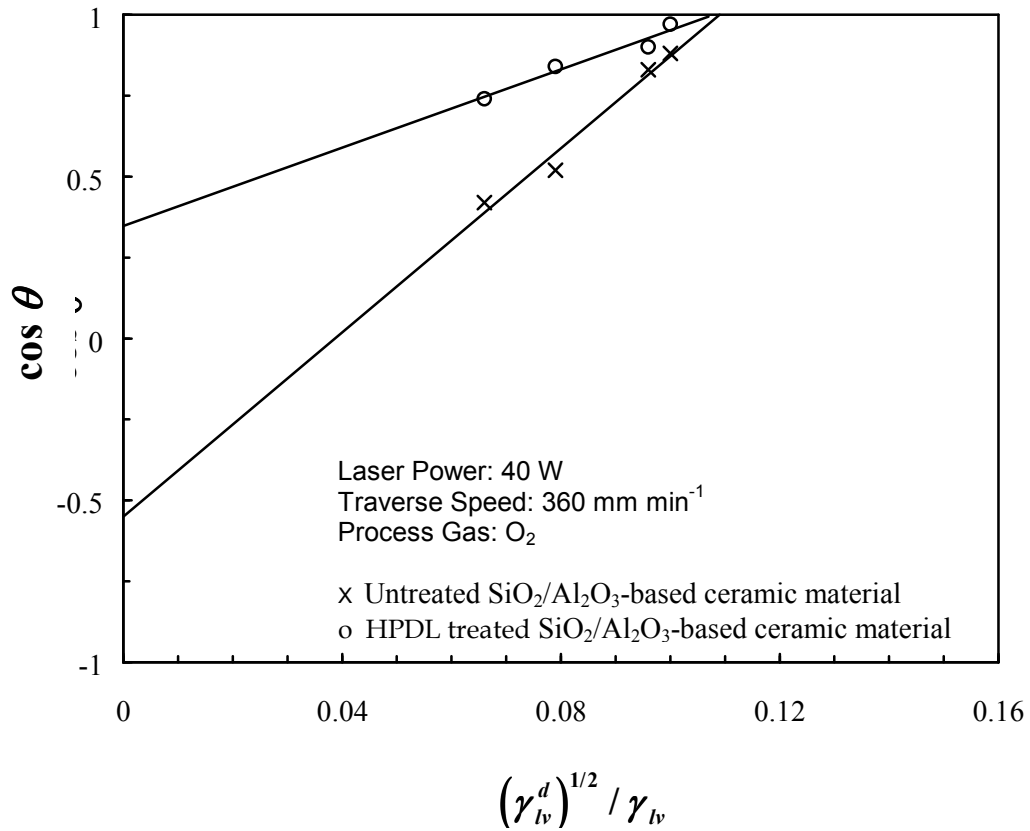


Figure 7

Typical SEM surface images of the $\text{SiO}_2/\text{Al}_2\text{O}_3$ -based ceramic material (a) untreated and (b) after HPDL surface treatment (40 W laser power, 360 mm min^{-1} traverse speed and O_2 process gas).

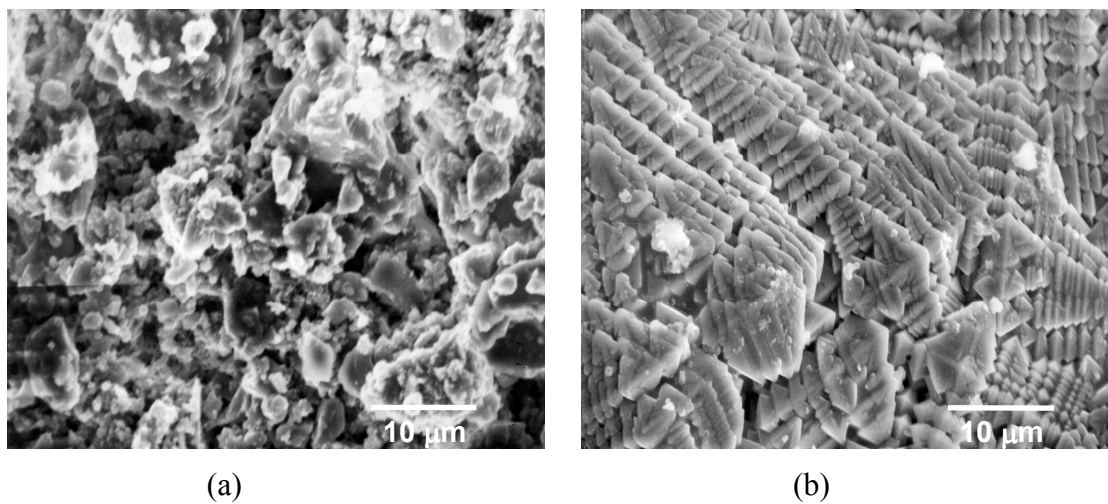


Figure 8

XRD analysis of the $\text{SiO}_2/\text{Al}_2\text{O}_3$ -based ceramic material before (bottom) and after (top) HPDL surface treatment (40 W laser power, 360 mm min^{-1} traverse speed and O_2 process gas).

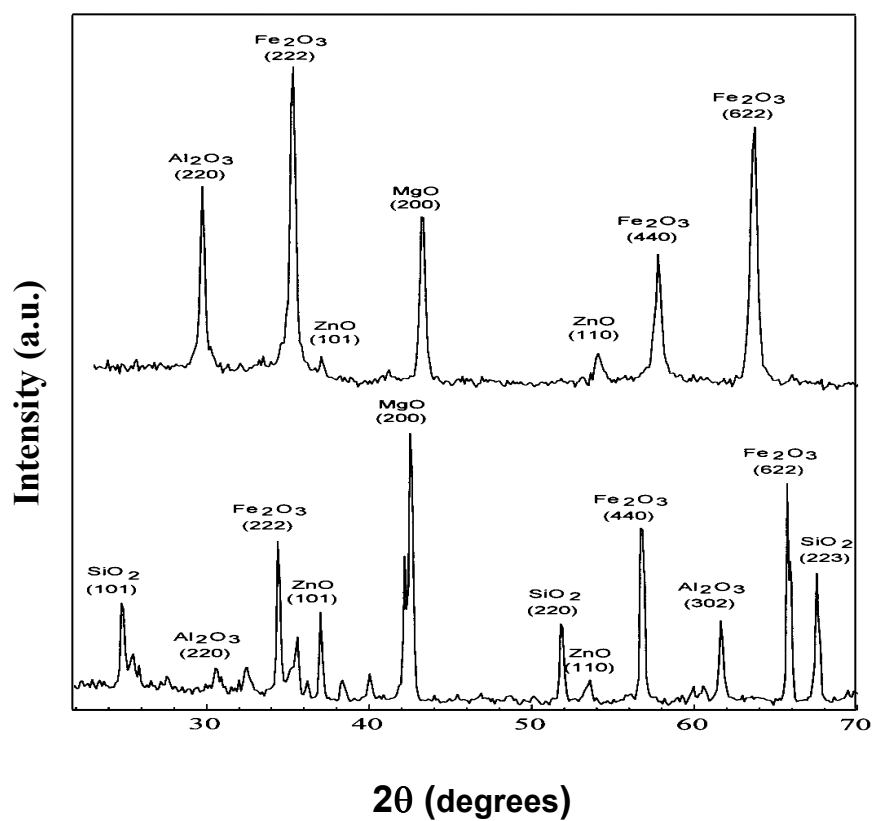


Figure 9

Relationship between solidified (20°C) enamel contact angle (θ) on the HPDL surface treated SiO₂/Al₂O₃-based ceramic material and HPDL energy density.

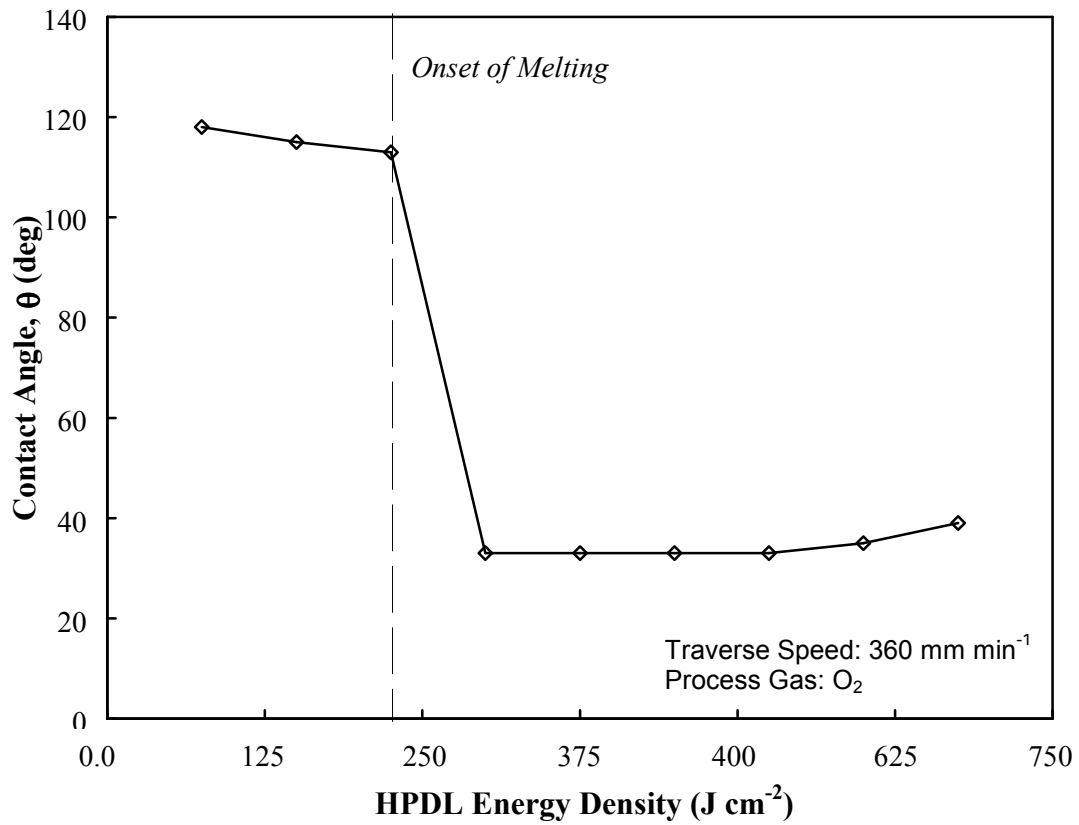


Table 1

Total surface energy (γ_{lv}) and the dispersive (γ_{lv}^d) and polar (γ_{lv}^p) components for the selected test liquids (Gutowski *et al.* 1992).

Liquid	γ (m Jm⁻²)	γ_{lv}^d (m Jm⁻²)	γ_{lv}^p (m Jm⁻²)
Human Blood	47.5	11.2	36.3
Human Blood Plasma	50.5	11.0	39.5
Glycerol	63.4	37.0	26.4
4-Octonol	27.5	7.4	20.1

Table 2

Mean values of contact angle (θ) formed between the selected control test liquids at 20°C and the SiO₂/Al₂O₃-based ceramic material before and after HPDL surface treatment (40 W laser power, 1500 mm min⁻¹ traverse speed and O₂ process gas).

Control Test Liquid	Contact Angle, θ (deg)	
	Untreated	HPDL Treated
Human Blood	61	37
Human Blood Plasma	64	38
Glycerol	34	28
4-Octanol	29	26

Table 3

Surface roughness values (Ra) of the SiO₂/Al₂O₃-based ceramic material before and after interaction with the HPDL in the various process gas environments (40 W laser power and 1500 mm min⁻¹ traverse speed).

Surface Roughness, Ra (μm)			
Untreated	Ar	N ₂	O ₂
25.9	6.6	6.4	6.3

Table 4

Determined surface energy values for the SiO₂/Al₂O₃-based ceramic material before and after HPDL irradiation (40 W laser power, 360 mm min⁻¹ traverse speed and O₂ process gas).

Surface Energy Component	SiO ₂ /Al ₂ O ₃ -based Ceramic Material Condition	
	Untreated	HPDL Treated
Dispersive Component, γ_{sv}^d	84.16 mJ/m ²	89.04 mJ/m ²
Polar Component, γ_{sv}^p	2.00 mJ/m ²	25.87 mJ/m ²
Total Surface Energy, γ_{sv}	86.16 mJ/m ²	114.91 mJ/m ²